Statistical projections of the mean changes in intra-seasonal rainfall characteristics over Zambia from the reference period 1971-2000 to the future 2021-2050.

Nephat Mwanza[1*◕], Suman Jain[1◕]

1 Department of Mathematics, Statistics and Actuarial Science, School of Natural and Applied Sciences. University of Zambia, Lusaka, 10101, Zambia.

◕These authors contributed equally to this work.
* Corresponding author: nephatmwanza@gmail.com

Abstract

As the Earth continues to warm, extreme seasonal precipitation events such as dry spells, floods, and droughts are expected to become more frequent and severe worldwide, including in Zambia. Zambia's agricultural sector, heavily dependent on seasonal rainfall, is highly sensitive to such fluctuations, with longer dry spells and floods threatening farmer livelihoods and national food security. This study investigates potential changes in intra-seasonal rainfall characteristics over Zambia from 1971-2000 to 2021-2050 using an ensemble of 22 experiments from the Coordinated Regional Climate Downscaling Experiment (CORDEX). Model performance in reproducing monthly climatology, spatial climatology, and inter-annual variability of rainfall was evaluated against the Global Precipitation Climatology Centre (GPCC; 1982-2000) observational dataset. The RCM simulations reasonably captured the monthly and spatial climatology of Zambian rainfall, with individual models exhibiting wet or dry biases, while the ensemble mean showed better agreement with observations than any individual model. Projections for 2021-2050 relative to the 1971-2000 baseline indicated a statistically significant median increase of 0.6 and 1.85 days in consecutive dry days (CDD) over JFM and OND, respectively, alongside a median reduction of 1.1 and 0.95 days in consecutive wet days (CWD) over the same seasons. The greatest projected increases in CDD occurred in Southern, Lusaka, Eastern, and Western provinces, whereas the projected reduction in CWD was more evenly distributed nationwide. These findings have important implications for Zambia's rain-fed agriculture: longer dry spells and flash floods during critical periods such as JFM may reduce crop yields and undermine food security. The projections presented here offer agricultural scientists and policymakers the spatially resolved evidence needed to design adaptation strategies tailored to Zambia's changing rainfall patterns.

Keywords: CORDEX, regional climate models, maximum number of consecutive dry days (CDD), maximum number of consecutive wet days (CWD), RCP8.5

Author summary

Zambia's agriculture depends heavily on seasonal rainfall, which is now becoming more unpredictable due to climate change. Farmers are facing longer dry spells and sudden floods that threaten crop production and national food security. To help understand what the future may look like, this study used climate models to project changes in rainfall patterns, focusing on the length of dry and wet periods across the country.

We analyzed simulations from 22 climate experiments to see how long stretches without rain (called consecutive dry days) and stretches of rainy days (consecutive wet days) might change by the year 2050. The results show that dry periods are likely to become longer, especially in southern and eastern Zambia. At the same time, wet periods are projected to become shorter.

These findings can support farmers, planners, and policymakers in designing adaptations to changing climate.

Introduction

Since the last century, the Earth's surface temperature has risen by approximately 1°C, largely driven by increased anthropogenic greenhouse gas (GHG) emissions from industrial, transportation, agricultural, and deforestation activities [1, 2]. This global warming trend has intensified the hydrological cycle, increasing the frequency, intensity, and duration of extreme weather events such as droughts, floods, and heat waves [3, 4]. These changes pose substantial risks to global food systems, infrastructure, human health, and ecosystems. Particularly in developing regions such as sub-Saharan Africa, the adaptive capacity remains low, exacerbating vulnerability to climatic extremes.

Regional Climate Models (RCMs), particularly those from the CORDEX-Africa framework, offer simulations of temperature and precipitation at a finer resolution (approximately 50 km) suitable for localized climate change impact studies [10, 11]. The Coordinated Regional Downscaling Experiment (CORDEX) enables ensemble modeling that enhances the reliability of regional climate simulations. Numerous studies have evaluated the capacity of RCMs to reproduce historical rainfall patterns across Africa, with results showing that while model biases persist, ensemble means often outperform individual simulations in reproducing observed rainfall variability [12–18]. Indices developed by the Expert Team on Climate Change Detection and Indices (ETCCDI), such as consecutive dry days (CDD) and consecutive wet days (CWD), are widely used to monitor and project climate extremes that influence flood and drought risk [19–21].

Emerging multi-model ensemble studies consistently project that, under high-emission scenarios like RCP8.5, Southern Africa will experience an increase in CDD and a decrease in CWD [22–24]. These trends suggest a shortening of the rainy season due to delayed onset, early cessation, and increased intra-seasonal dry spell duration [25, 26]. In Zambia, these changes are already evident: recent studies report increased dry spell frequency, shortened seasons, and reduced seasonal rainfall totals, particularly in southern and central provinces [27–29]. Given that over 70% of Zambia's population relies on rain-fed agriculture, such shifts present critical risks to food security, water availability, and rural livelihoods [30, 31].

Despite growing concern, there remains a significant gap in high-resolution, country-specific analyses of rainfall extremes over Zambia using the CORDEX RCM ensembles. Existing literature has largely focused on historical trends or regional aggregates, limiting their utility for sub-national adaptation planning.

Moreover, even within the newer CMIP6 generation of global climate models, studies continue to report a wide inter-model spread and a widespread wet bias in simulating Zambia's summer rainfall, linked to an overly intensified simulated Inter-Tropical Convergence Zone and strengthened cross-equatorial moisture transport [57]. Bias-correction assessments of CMIP6 ensembles over Southern Africa likewise show persistent difficulty in representing extreme precipitation indices such as CDD [56]. These ongoing limitations at the global-model scale reinforce the continued value of dynamically downscaled, multi-RCM CORDEX ensembles of the type used in this study for producing spatially resolved, sub-national projections of rainfall extremes.

This study addresses this gap by using daily precipitation outputs from 22

CORDEX-Africa RCM simulations under the RCP8.5 scenario to (1) evaluate model performance in simulating observed rainfall climatology and variability, (2) project future changes in CDD and CWD over Zambia for the period 2021–2050 relative to the 1971–2000 baseline, and (3) spatially identify hotspots of change. The findings aim to support evidence-based adaptation policies by providing robust, spatially resolved projections of rainfall extremes most relevant to Zambia's agriculture and climate resilience planning.

Materials and methods

Study Region

Geographical location and topography

Zambia is a landlocked country located in Southern Africa, bounded by the Democratic Republic of Congo to the north, Tanzania to the northeast, Malawi to the east, Mozambique to the southeast, Namibia to the southwest, and Angola to the west. Geographically, it lies between longitudes 22°E and 34°E, and latitudes 8°S and 18°S [32]. The country's total area is approximately 752,614 km^2 [33], mostly consisting of high plateaus ranging from 950 to 1,500 meters above sea level

Climate and agro-ecological zones

According to the Köppen climate classification, Zambia has a humid sub-tropical climate [34]. The country is characterised by three main seasons: the rainy season (November to April), the dry season which is subdivided into the cool dry winter season (May to July), and the hot dry summer (August to October) [32, 35]. The rains in Zambia are strongly influenced by the movement of the Inter-Tropical Convergence Zone (ITCZ) as well as the EL Nino/Southern Oscillation (ENSO) phenomenon [36]. The highest amount of rainfall is received by the northern part of the country ($>$ 1000 mm/season). Seasonal rainfall total keeps decreasing towards the southern parts of the country with seasonal total rainfall $<$ 800 mm. This gradient in the rainfall regime divides the country into three Agro Ecological zones, as shown in Fig 1.

Fig 1. Agro-ecological zones of Zambia. Zambia is divided into three agroecological zones based on rainfall distribution and elevation. Zone I (southern Zambia) is the driest and most drought-prone. Zone II covers the central region with moderate rainfall, while Zone III in the north receives the highest rainfall. Zambia's location in Africa is indicated by the blue color in the map of Africa. [37]

Data types and their sources

This study utilized two primary sources of precipitation data: (i) dynamically downscaled climate model simulations from the CORDEX-Africa archive `https://esgf-data.dkrz.de/search//cordex-dkrz/` [26], and (ii) observed gridded rainfall data from the Global Precipitation Climatology Centre (GPCC)`http://gpcc.dwd.de` [39]. Both datasets are publicly available under a Creative Commons Attribution 4.0 International License (CC BY 4.0).

Climate model simulations

The climate models simulated daily data for the domain Zambia for the baseline period 1971-2000 and future period 2021-2051 was extracted from the CORDEX Africa database. Six CORDEX Regional Climate Models (RCMs) downscaled 12 global climate models (GCMs) of the Coupled Model Intercomparison Project (CMIP5). The 6 RCMs utilised include: RCA, HIRHAM, CCLM, RACMO, REMO, and CRCM, the inclusion was based on their availability within an ensemble of experiments provided by CORDEX Africa at the time of download. From 6 CORDEX RCMs and 12 GCMs from CMIP5, 26 GCM-RCM simulations with complete historical (1971-2000) output were available at 0.44°(50 km) resolution over the CORDEX Africa domain and were used for the historical climatology and variability evaluation (Figs 2–5). Of these, 22 simulations also had complete future (2021-2050) RCP8.5 output and were used for the CDD/CWD projection analysis. The CORDEX RCMs were driven by the Representative Concentration Pathway 8.5 (RCP8.5) scenario. RCP8.5 is preferred as it comprises the largest ensemble (25 runs) and, may be considered as the most realistic business-as usual scenario given the current trajectory of global greenhouse gas emissions [40].

Observational rainfall data

Monthly gridded gauge-based rainfall data for the period 1982-2000 at grid resolution of 50 kms by 50 kms was utilized in this study. The data was acquired from the Global Precipitation Climatology Centre (GPCC). GPCC is operated by the German Weather Service (Deutscher Wetterdienst, DWD).

Methods

Assessment of model simulations against observation

A number of metrics were computed to evaluate the ability of CORDEX RCMs in simulating the main characteristics of rainfall in Zambia. These metrics include the comparisons in: (i) mean monthly climatology of rainfall, (ii) spatial distribution of mean seasonal rainfall, (iii) inter-seasonal variability. Daily rainfall for all 22 downscaled experiments were extracted from 1 October to 31 March for the years 1982 to 2000 for a spatial region covering Zambia.

The ensemble mean was computed as studies have shown that in certain regions individual RCMs simulate precipitation patterns poorly [15], whereas the ensemble mean is found to be a better fit for the data [12–14, 17]. GPCC daily rainfall data was extracted from 1 October to 31 March for period 1982 to 2000 over the same region as for RCMs.

To detect differences between seasonal total mean rainfall of the model simulations and the observed GPCC, a paired Student's t test was applied individually for seasons OND and JFM.

Projection of changes in the longest consecutive dry days period and longest consecutive wet days period

A day is classified as dry or wet. A dry day is a day on which accumulated rainfall is less than 1 mm. In this study, two precipitation indices are investigated, longest consecutive dry days spell (CDD) and longest consecutive wet days spell (CWD), defined by the Expert Team on Climate Change Detection and Indices (ETCCDI) [19].

The two indices were computed annualy for the seasons, October, November and December (OND) and January, February and March (JFM) after daily rainfall was spatially averaged over the region covering Zambia. Further the climatological mean of the CDD and CWD for the future period (2021-2050) and reference period (1971-2000) from each model simulation are displayed as box-and-whisker plots (S1 Fig). From the same computations, the projected changes in CDD and CWD were calculated as:

$$\Delta I_i = I_{i,f} - I_{i,r} \tag{1}$$

for $i = 1, 2, \cdots 26, \quad f = 2021 - 2050$ and $r = 1971 - 2000$, where $I_{i,f}$ represents the future climatological mean and $I_{i,r}$ the climatological mean of the reference period. Box-and-Whisker plots were further used to plot the changes in CDD and CWD spanning all the simulation differences for the two seasons.

To quantify the changes in CDD and CWD, the Wilcoxon Paired Signed Rank (WPSR) nonparametric test was applied to the seasonal values for the future period and reference period at 0.05 level of significance under the hypothesis $H_\circ$: the median of the number of days of CDD (CWD) for the future period is equal to that of the reference period, against the alternative H_1 : the median of the number of days of CDD (CWD) for the future period has changed with respect to reference period.

The WPSR test was utilized in Nkemelang et al [43] to determine the significance of changes in various climate indices over Botswana. A nonparametric method was chosen because it would be problematic or inaccurate to try to summarize the data into a single number (like a mean) due to the nature of the variables being measured (CDD and CWD). A parametric paired t-test was also performed to test the significance of mean change in CDD and CWD.

The distribution of the changes in CDD and CWD across Zambia was further analyzed visually to identify the hotspots. To achieve this, the ensemble mean of the models that agreed on the sign of the change was utilized. The criterion for the robustness of climate change signal that was adopted is more than 80% of model agreement on the sign of change [22, 40, 44].

Results

Performance of CORDEX RCMs simulations over Zambia

The mean monthly climatology

To evaluate how well the CORDEX-Africa Regional Climate Models (RCMs) simulate Zambia's seasonal rainfall, we analyzed the average monthly rainfall over the historical period (1982–2000). Due to the number of simulations (22 models), results are presented in three panels in Fig 2, comparing each model and the ensemble mean against the observed GPCC data.

Zambia has a single rainy season that typically begins in late October and peaks in January. Most of the models captured the overall shape of this seasonal rainfall cycle well. This is supported by results from the Taylor diagram in Fig 2 (d), where all models showed strong correlation (above 0.9) with the observed GPCC data.

However, there were differences in the strength (amplitude) and timing of rainfall. Some models showed too much rain at the beginning of the season (October–December), suggesting an early onset. While most models correctly identified January as the peak rainfall month, others shifted the peak to November, December, or February. Models M22 and M26 peaked in November, while M1, M2, M5, M8, M11, M12, M18, M20, M21, and M25 peaked in December. M23 delayed the peak to February, and M10 and M24 showed two peaks; one in December and another in February.

Most models correctly simulated the dry season (May–September), though M1 and M23 slightly overestimated rainfall during this period. While some models performed well across all months, such as M3, M6, M7, M9, M13, M14, M15, M16, M17, and M19, while others (M4, M10, M12, M18, M20, M22, M24, M25, and M26) struggled to match the observed monthly pattern. Interestingly, most of the lower-performing models used the RCA4 regional climate model (see S1 Table).

Overall, the ensemble mean closely matched the observed monthly rainfall pattern and outperformed individual models, confirming its usefulness in representing Zambia's annual rainfall cycle.

Fig 2. Mean monthly annual cycle of rainfall over Zambia from 22 CORDEX simulations, the ensemble mean, and observed GPCC data. (a–c) Time series of monthly rainfall climatology comparing 22 RCM simulations, ensemble mean, and GPCC observations, grouped across three panels for clarity. (d) Taylor diagram showing model performance in reproducing the annual rainfall cycle, based on correlation, normalized standard deviation, and centered RMS difference with respect to GPCC. Each number represents a model simulation.

Visual inspection of spatial climatology

To assess the spatial performance of the CORDEX RCMs, Figs 3 and 4 present maps of the mean seasonal rainfall for the JFM and OND seasons, respectively, over the period 1982–2000. These figures display the observed GPCC rainfall climatology, the ensemble mean, and outputs from each of the 22 individual model simulations.

Fig 3. Spatial climatology of rainfall over Zambia during the JFM season for 22 model simulations, the ensemble mean, and the observed GPCC data. Each subplot displays the spatial distribution of mean seasonal rainfall for the period 1982–2000. The figure illustrates the ability of individual CORDEX RCM simulations and the ensemble mean to capture spatial rainfall patterns over Zambia, as compared to GPCC observations.

Fig 4. Spatial climatology of rainfall over Zambia during the OND season for 22 model simulations, the ensemble mean, and the observed GPCC data. Each subplot displays the spatial distribution of mean seasonal rainfall for the period 1982–2000. The figure illustrates the ability of individual CORDEX RCM simulations and the ensemble mean to capture spatial rainfall patterns over Zambia, as compared to GPCC observations.

Consistent with established climatology, Zambia receives higher rainfall in the northern region, with a gradual decrease toward the south, a gradient strongly influenced by the seasonal migration of the Inter-Tropical Convergence Zone (ITCZ). Most model simulations successfully captured this north–south rainfall gradient in both seasons, reflecting reasonable skill in simulating the spatial distribution of precipitation across Zambia. Despite this general agreement, spatial biases were evident. Some models, particularly M11 and M23, substantially underestimated rainfall across nearly all regions in both the JFM and OND seasons. Conversely, several models—especially those utilizing the RCA4 regional climate model (M2, M4, M5, M10, M12, M14, M18, M22, M24, M26)—exhibited overestimation of rainfall, particularly over eastern Zambia. These patterns of overestimation by RCA4-based models were consistently observed across both seasons.

Given the spatial heterogeneity of model performance, further statistical evaluation was conducted. Seasonal total rainfall from each simulation and the ensemble mean was compared to the GPCC reference using a paired Student's t-test. The null hypothesis assumed no significant difference in mean rainfall between model outputs and observations, tested at a 5% significance level. The results of the statistical analysis are summarized in Table 1. In the OND season, nearly all simulations indicated a wet bias relative to GPCC, with the exception of M1 and M23. All wet biases, except for M1 and M6, were statistically significant. In contrast, JFM rainfall showed more variability: over half the simulations (including EnsMean, M1, M2, M5, M7, M12, M15, M17, M18, M20, M21, M23, M25, M26) displayed a dry bias, while others showed a wet bias. Significant biases were observed for models M1, M2, M3, M6, M10, M12, M14, M15, M17, M23, and M24. Models M1 and M23 consistently demonstrated dry biases in both seasons, with M23 showing particularly large deviations from observations. These biases were statistically significant in both JFM and OND for M23, further reinforcing its consistent underperformance.

Additional insights from the supporting information for seasonal mean total rainfall values of JFM and OND over Zambia from each model simulation and the observed GPCC S2 Table indicate that M23 simulated the lowest seasonal rainfall totals—130.1 mm in OND and 211.8 mm in JFM—compared to the observed GPCC values of 333.9 mm and 527.1 mm, respectively. The simulation with the highest JFM rainfall was M14 (610.2 mm), while M4 recorded the highest OND value (526.4 mm). However, most simulations produced rainfall values within a close range of the observed GPCC, especially during the JFM season, supporting the general reliability of the ensemble for spatial climatology analysis.

Inter-seasonal variability

Interannual variability of seasonal total rainfall was evaluated using Taylor diagrams (Fig 5), following the approach of [12] and [13]. Fig 5 illustrates the degree to which each of the 26 model simulations and the ensemble mean replicate the year-to-year variability of seasonal mean rainfall over Zambia for the period 1982–2000, across the two rainfall seasons: JFM and OND.

In both seasons, the RCM simulations show a weak ability to reproduce the interannual variability captured by GPCC observations. During JFM, over half of the models exhibit correlation coefficients between –0.4 and 0, indicating a poor match with observed interannual fluctuations. In the OND season, while more than 80% of the models have positive correlations, most fall below 0.4, suggesting only modest improvements over the JFM season.

The root-mean-square error (RMSE) is generally higher in JFM compared to OND. All models in the JFM season record an RMSE above 60 mm, while in OND, most models fall above 40 mm—with the exception of M23 and the ensemble mean (M27). Notably, the ensemble mean exhibits a consistently lower standard deviation in both seasons, indicating underestimation of variability relative to GPCC.

Model-specific performance also varies. Simulations M1, M3, M6, M9, M10, M11, M15, M16, M17, M21, M23, and the ensemble mean (M27) demonstrate consistently limited variation compared to GPCC across both seasons. In OND, M23 stands out with the strongest correlation (0.542) and the lowest standard deviation among all simulations. Conversely, M13 shows the largest variability (standard deviation of 66.28 mm and a correlation of –0.061), although it is not clearly represented in the diagram. Model M24 also displays significant variability (61.04 mm), while M20 records the highest RMSE in OND (above 80 mm). In contrast, during JFM, all model simulations underestimate variability relative to GPCC, with generally weak correlations and greater RMS errors. These patterns are consistent with results from previous studies indicating the difficulty of capturing seasonal variability over Southern Africa.

Overall, the CORDEX RCMs show limited skill in reproducing observed interannual variability of seasonal rainfall over Zambia. The ensemble mean generally outperforms individual models in terms of reduced RMSE and bias, though it also underrepresents variability when compared to the observational reference.

Table 1. Differences in Seasonal Mean Rainfall Between Model Simulations and GPCC Observations During JFM and OND.

Model Comparison	*t*-Statistic		*p*-Value (Two-Tailed)	
	JFM	OND	JFM	OND
Ensmean-GPCC	-2.41	**5.26**	0.027	<.001
M1-GPCC	**-5.80**	-1.88	<.001	0.076
M2-GPCC	**-2.83**	**5.90**	0.011	<.001
M3-GPCC	**2.84**	**9.36**	0.011	<.001
M4-GPCC	0.62	**15.60**	0.542	<.001
M5-GPCC	-2.35	**4.33**	0.030	<.001
M6-GPCC	**2.48**	1.18	0.023	0.253
M7-GPCC	-0.11	**2.45**	0.912	0.025
M8-GPCC	0.03	**6.80**	0.980	<.001
M9-GPCC	0.97	**6.10**	0.346	<.001
M10-GPCC	**2.71**	**13.42**	0.014	<.001
M11-GPCC	0.19	**9.03**	0.852	<.001
M12-GPCC	**-4.56**	**8.00**	<.001	<.001
M13-GPCC	1.49	**2.79**	0.153	<.001
M14-GPCC	**3.74**	**5.67**	0.001	<.001
M15-GPCC	**-3.15**	**2.56**	0.006	0.0198
M16-GPCC	0.19	**12.53**	0.851	<.001
M17-GPCC	**-3.92**	**4.23**	<.001	<.001
M18-GPCC	-0.71	**11.16**	0.484	<.001
M19-GPCC	0.92	**3.35**	0.371	0.0036
M20-GPCC	-1.55	**4.67**	0.139	<.001
M21-GPCC	-1.69	**6.40**	0.108	<.001
M22-GPCC	1.60	**9.67**	0.126	<.001
M23-GPCC	**-15.81**	**-25.56**	<.001	<.001
M24-GPCC	**2.93**	**7.56**	0.009	<.001
M25-GPCC	-0.11	**12.95**	0.913	<.001
M26-GPCC	-0.35	**9.27**	0.732	<.001

Bold values indicate statistically significant differences at the 0.05 level based on a paired two-tailed Student's t-test.

Fig 5. Taylor diagrams for JFM (top) and OND (bottom) seasons, based on the interannual variation of seasonal mean precipitation for the period 1982–2000 over Zambia. Each number corresponds to a specific model simulation, showing its correlation coefficient, standard deviation, and centered root mean square difference relative to GPCC observations. The diagrams visualize how well each model captures the year-to-year variability of seasonal rainfall.

Consecutive dry days and consecutive wet days

The precipitation indices: CDD and CWD—were computed for the OND and JFM seasons using daily precipitation data from 22 CORDEX-Africa simulations under the RCP8.5 scenario. The analysis compared the climatological means for the historical baseline period (1971–2000) and the projected future period (2021–2050).

Fig 6 presents box-and-whisker plots of projected changes in CDD and CWD, calculated as the difference between future and baseline seasonal means. The projections indicate a consistent increase in the mean CDD and a corresponding decrease in the mean CWD across both seasons. Specifically, at least 80% of the model simulations project an increase in CDD and a reduction in CWD for both OND and JFM seasons—meeting the threshold for robust multi-model agreement as defined in recent literature [22, 40, 44].

The changes are statistically significant at the 0.05 level, as confirmed by both the Wilcoxon Signed-Rank Test and the paired Student's t-test (Table 2). In terms of central tendency, the median increase in CDD is estimated at 1.85 days for OND and 0.6 days for JFM. Conversely, the median reduction in CWD is 1.1 days in JFM and 0.95 days in OND. These results suggest that Zambia is likely to experience longer dry spells and shorter wet spells during both rainfall seasons under a high-emissions trajectory.

The projected increase in CDD is notably more pronounced during the OND season, which coincides with the onset of the rainy season. This pattern is likely linked to increased variability in rainfall onset, contributing to longer dry stretches at the start of the agricultural calendar. In contrast, the JFM season exhibits a narrower range of changes in CDD, suggesting more stable dry spell patterns during the core of the rainy season.

In the case of CWD, the JFM season shows a wider range of projected reductions compared to OND, likely due to increased uncertainty in rainfall cessation timing and intra-seasonal rainfall variability in the latter half of the rainy season.

Fig 6. Projected changes in CDD and CWD for OND and JFM seasons. Box plots showing projected changes in the number of Consecutive Dry Days (CDD) and Consecutive Wet Days (CWD) over the period 2021–2050 relative to the baseline period 1971–2000. Results are based on 22 model simulations for the OND and JFM seasons.

Table 2. Statistical values of the Wilcoxon signed-rank test and the Student's paired t-test based on 22 ensemble members. Bold values indicate significance at the 0.05 level.

Variable	Season	Wilcoxon statistic	One-sided p-value	t-test statistic	One-sided p-value
CDD	OND	**226.0**	$< .001$	**6.49**	$< .001$
CDD	JFM	**227.0**	$< .001$	**3.984**	$< .001$
CWD	OND	**25.0**	$< .001$	**-5.112**	$< .001$
CWD	JFM	**23.5**	$< .001$	**-4.312**	$< .001$

Wilcoxon signed-rank and Student's paired t-test results for projected changes in consecutive dry days (CDD) and consecutive wet days (CWD) under RCP8.5 scenario across OND and JFM seasons.

Visual inspection of the changes in CDD and CWD

Fig 7 and Fig 8 show the spatial distribution of changes in the mean CDD and mean CWD over Zambia for the period 2021-2050 from the baseline period 1971-2000 for the OND and JFM seasons, respectively. For CDD, changes in the season JFM are evenly distributed across the country, with certain regions having about 0.6-1.2 days as the highest. However, in the OND season the highest number of changes in CDD are in the southern part of the country. These changes in CDD are observed in provinces such as Southern, Lusaka, Western, Eastern, and parts of Central, with days ranging from 2.5 to 5 days. Further, in both seasons parts of Southern province consistently have greatest increase in CDD. On the other hand a reduction in the number of CWD is more evenly distributed across the country, with only parches in certain regions with more(less) the number of CWD in both seasons. The changes in the number of CWD ranges 0-8 days in JFM and 0-5 days in OND season.

In Fig 7(b), the projected changes in CDD show an increase of 0-2.5 days in North-Western, Copperbelt, Luapula, Northern and Muchinga provinces. The projected

Fig 7. Spatial distribution of mean CDD and CWD over Zambia for the OND season.
Top row: Mean CDD for the control period (1971–2000) and projected changes for the future period (2021–2050).
Bottom row: Mean CWD for the control period (1971–2000) and projected changes for the future period (2021–2050).

increase in CDD is greater in Western, Southern, Lusaka, Eastern and Central provinces, with 2.5 – 5.0 days.

For CWD, Fig 7(d) shows that the projected changes indicate a reduction of 0-5 days across the country, with only small portions of Central/Southern provinces showing a reduction of 5-10 days while small portions of Northern/Muchinga show an increase of 0-5 days.

Fig 8. Spatial distribution of mean CDD and CWD for Zambia. Top row: Mean CDD during JFM for the control period (1971–2000) and projected changes for the future period (2021–2050).
Bottom row: Mean CWD during JFM for the control period (1971–2000) and projected changes for the future period (2021–2050).

In Fig 8(b), the projected changes in CDD during JFM indicate an increase of 0-0.6 days across most parts of the country. However some parts of Southern, Central and Eastern show an increase of 0.6-1.2 days.

The projected changes in CWD in Fig 8(d) indicate a reduction of 0-8 days in most parts of the country. While parts of Central province indicate an increase of 0-8 days.

Discussion

This study aimed to assess intra-seasonal rainfall extremes—specifically consecutive dry days (CDD) and consecutive wet days (CWD)—over Zambia using an ensemble of 22 CORDEX-Africa Regional Climate Model (RCM) simulations. Before interpreting future projections, it was essential to evaluate how well these RCMs reproduced historical rainfall climatology and variability, and then explore the implications of their future projections for Zambia's agriculture and climate adaptation planning.

The performance assessment revealed that most RCMs, despite some biases, adequately captured the mean monthly climatology and spatial distribution of rainfall over Zambia. These biases were also reported by Kalognomou et al. [12] and Endris et al. [13] for Southern Africa and Eastern Africa domains respectively. Some RCMs, particularly those downscaled using RCA4, exhibited wet biases during the early part of the rainy season (OND), consistent with the findings of Nikulin et al. [11]. For the HIRHAM5-NorESM1_M model, results confirm the findings by Warnatzsch and Reay [15] that it greatly underestimates rainfall during the wet season. The interannual variability of rainfall, especially in the JFM season, was not well captured, with several models showing low or even negative correlation with observed GPCC data. This aligns with previous work by Kalognomou et al. [12], indicating persistent challenges in modeling year-to-year variability in Southern Africa. However, the ensemble mean exhibited high correlation with the GPCC dataset, particularly for the annual rainfall cycle. This is consistent with results from other studies [11, 13–18].

The projected changes in Zambia's intra-seasonal rainfall characteristics, particularly the increase in CDD and the decrease in CWD, reflect a broader regional trend consistent with recent findings across Southern Africa. Our analysis under the RCP8.5

scenario suggests that Zambia will experience statistically significant lengthening of dry spells and shortening of wet spells during both OND and JFM seasons between 2021–2050 compared to the historical baseline of 1971–2000. These results are in line with those of Libanda and Ngonga [29] for the period 2021–2100 compared to the baseline period 1961–1990, and other prior studies eg [28, 45]. These findings have important implications, particularly for Zambia's agriculture, which is heavily reliant on seasonal rainfall and is therefore highly vulnerable to changes in intra-seasonal precipitation extremes.

The observed trends of increasing CDD and decreasing CWD in this study are in strong agreement with multi-model assessments such as those by Samuel et al. [24], who found similar patterns across major Southern African river basins under multiple global warming levels using CMIP5, CMIP6, CORDEX, and CORE ensembles. These changes persist under all warming levels (1.5 °C, 2.0 °C, and 3.0 °C), emphasizing their robustness and potential to challenge regional water and food security. Our results also align with Maúre et al. [22], who projected intensification of dry extremes and a decline in wet spell duration across Southern Africa at both 1.5 °C and 2.0 °C warming levels. Likewise, Pinto et al. [23] and Giorgi et al. [46] reported increases in CDD over Southern Africa by century-end under high-emission scenarios, consistent with trends in our Zambia-focused analysis. New et al. [47] had earlier identified statistically significant increases in dry spell duration and rainfall intensity across the region over the late 20th century.

The mechanisms driving these trends are consistent with large-scale atmospheric dynamics. Shongwe et al. [48] and Rouault et al. [49] observed that changes in the ITCZ position, weakened Indian Ocean moisture flux, and ENSO-related anomalies contributed to shortened rainy seasons. Zita et al. [50] emphasized the roles of ENSO, IOD, and TAV in modulating extreme rainfall patterns in sub-Saharan Africa. A recent comprehensive review by Munday et al. [55] similarly attributes much of the inter-model diversity in Southern African rainfall projections to differences in the representation of moisture transport and convective processes across models, reinforcing the value of multi-model ensemble approaches such as the one adopted here. These mechanisms help explain the spatial and seasonal heterogeneity seen in Zambia's projections. The greatest projected increase in CDD during OND was observed in Southern, Lusaka, Western, Eastern, and parts of Central provinces, consistent with earlier results [22, 23, 29].

The agricultural and socio-economic implications of these projections are significant. Zambia's rain-fed agriculture is sensitive to rainfall timing and distribution. Ngoma et al. [31] projected that rainfall reductions and increased variability would lower crop yields, GDP, and household welfare—particularly in regions where our study projects the largest increase in CDD. Chemura et al. [51] noted that CDD and CWD are stronger predictors of crop suitability than seasonal totals; when included in maize suitability models, these indices showed more severe reductions across southern Africa under future climates.

These findings underscore the urgent need for robust adaptation strategies. Ayanlade et al. [52] highlight the importance of improved technology transfer to enhance resilience among smallholder farmers, including access to drought-resistant crops, moisture conservation techniques, and local climate services. Stadtbäumer et al. [53] illustrated how adaptive farm-level strategies such as altered land use and flexible cropping calendars can reduce climate vulnerability in rural Zambia. The spatially resolved projections from our study can guide more effective, targeted interventions.

Recent CMIP6 work by Bobde et al. [54] supports our findings by projecting an increased frequency of very dry years in Southern Africa, including Zambia, along with fewer but more intense rainfall events. These trends stress the importance of anticipatory planning and resilient infrastructure investment.

The severity of these projected changes was starkly illustrated by the 2023/24 rainfall season, when a Southern Africa-wide drought triggered national disaster declarations in Zambia, Zimbabwe, and Malawi, destroying an estimated 982,765 ha of the roughly 2.3 million ha of maize planted in Zambia and contributing to a 33% food inflation surge [58]. A rapid attribution analysis by World Weather Attribution [58] found that the strong 2023/24 El Niño event, rather than long-term anthropogenic warming, was the dominant driver of that particular season's rainfall deficit. This distinction matters: attribution of a single extreme season differs from the multi-decadal, scenario-based CDD/CWD trend detected in this study. Nevertheless, the 2023/24 drought offers a vivid, real-world illustration of the type of intensified dry-spell conditions in Southern, Lusaka, Western, Eastern, and Central provinces that our RCP8.5 projections indicate will become more frequent by 2021–2050, underscoring the urgency of the adaptation strategies discussed above.

Taken together, the evidence presented in this study confirms that Zambia is on a trajectory toward more extreme rainfall conditions. These changes will likely intensify, even under ambitious global mitigation scenarios. Strengthening institutional capacity, improving access to climate information, and developing localized interventions are essential to safeguard food security and livelihoods. As the climate signal strengthens, Zambia's adaptation strategies must be underpinned by high-resolution, ensemble-based projections such as those offered here.

Conclusion

This study assessed future changes in intra-seasonal rainfall extremes—consecutive dry days (CDD) and consecutive wet days (CWD)—over Zambia under the high-emissions RCP8.5 scenario for the periods 1971–2000 (baseline) and 2021–2050 (projection). An ensemble of 22 CORDEX-Africa simulations from six regional climate models (RCMs) driven by 12 global models was used. Model performance was evaluated against GPCC observational data, revealing that most simulations reasonably captured spatial rainfall patterns and the annual cycle, though seasonal variability and interannual fluctuations were underestimated, especially in the JFM season.

Projected changes show a statistically significant increase in CDD and a decrease in CWD, with the most pronounced increases in dry spells occurring in Southern, Lusaka, Eastern, and Western provinces. These findings suggest an elevated risk of drought conditions and shorter wet spells, with serious implications for Zambia's rainfed agriculture and food security.

To adapt effectively, Zambia must prioritize climate-resilient agricultural strategies, including investment in irrigation, enhanced climate monitoring infrastructure, and expanded access to climate data for research and planning. Further studies should evaluate higher-resolution models and additional rainfall characteristics such as onset and cessation dates. This research provides foundational evidence to support national adaptation planning and policy development in the face of a changing climate.

Supporting information

S1 Fig. Distribution of CDD and CWD across model simulations for the baseline and future periods. Box-and-whisker plots of Consecutive Dry Days (CDD) and Consecutive Wet Days (CWD) for the OND and JFM seasons, comparing the historical baseline period (1971–2000, His) and the future period (2021–2050, RCP8.5) across the 22 individual CORDEX-Africa model simulations. Unlike Fig 6, which shows the projected change (future minus baseline) for each simulation, this figure shows the absolute climatological distributions for each period, illustrating the spread across models before and after the projected shift.

S1 Table. Characteristics of the Regional Climate Models (RCMs) used in this study [11]. This table summarizes the core features of the six RCMs utilized in the CORDEX-Africa ensemble, including model developers, spatial configuration, physical parameterizations, and reference sources. These characteristics influence the ability of each model to simulate regional climate dynamics over Zambia.

S2 Table. Seasonal mean total rainfall values of JFM and OND over Zambia from each model simulation and the observed GPCC. This table presents domain-averaged seasonal rainfall totals (in mm) for the January–February–March (JFM) and October–November–December (OND) seasons. Values are provided for the observed GPCC dataset, the ensemble mean, and each of the 26 CORDEX-Africa model simulations. These values were computed over Zambia for the baseline evaluation period 1982–2000.

S3 Table. Mean values of CDD and CWD over the OND and JFM seasons for the baseline period (1971–2000) and future period (2021–2050). This table summarizes the climatological mean of Consecutive Dry Days (CDD) and Consecutive Wet Days (CWD) computed from the 22 model simulations for both OND and JFM seasons. The values represent domain-averaged rainfall indices across Zambia.

S4 Table. Median values of projected changes in Consecutive Dry Days (CDD) and Consecutive Wet Days (CWD) for the period 2021–2050 relative to the baseline 1971–2000. This table reports the median number of days by which CDD is projected to increase and CWD is projected to decrease in the January–February–March (JFM) and October–November–December (OND) seasons. The projections are based on an ensemble of 22 CORDEX-Africa RCM simulations under the RCP8.5 scenario.

Acknowledgments

First and foremost, I thank Yahweh for guidance, protection, and the gift of knowledge and wisdom throughout this journey.

I express my sincere gratitude to my supervisor, Mrs. Suman Jain, whose insightful guidance and encouragement were invaluable to this work.

Special thanks to Mr. Zilore Mumba for his assistance with climate data extraction.

I gratefully acknowledge the financial support received from the Eastern African Universities Mathematics Programme (EAUMP), which made this research possible.

I also acknowledge the support received from the Future Climate for Africa (FCFA) program, particularly the Python training workshops. I am thankful to the instructors—Maureen Ahiataku, Jeffrey Aryee, Marian Osei, and Leif Denby—for their excellent teaching and mentorship.

Finally, I extend my appreciation to my lecturers in the Department of Mathematics and Statistics at the University of Zambia—Dr. M. Lombe, Dr. I.D. Tembo, Dr. V.M. Nawa, Dr. A. Ngwengwe, Dr. A. Banda, and Dr. K. Muzundu —for providing me with the mathematical and statistical tools essential for this research.

References

1. IPCC. Climate Change 2014: Synthesis Report. Contribution of Working Groups I, II and III to the Fifth Assessment Report of the Intergovernmental Panel on Climate Change. [Core Writing Team, Pachauri RK, Meyer LA (eds.)]. Geneva, Switzerland: IPCC; 2014. 151 pp.

2. IPCC. Summary for Policymakers. In: Global warming of 1.5°C. An IPCC Special Report on the impacts of global warming of 1.5°C above pre-industrial levels and related global greenhouse gas emission pathways, in the context of strengthening the global response to the threat of climate change, sustainable development, and efforts to eradicate poverty. [Masson-Delmotte V, Zhai P, Pörtner HO, Roberts D, Skea J, Shukla PR, Pirani A, Moufouma-Okia W, Péan C, Pidcock R, Connors S, Matthews JBR, Chen Y, Zhou X, Gomis MI, Lonnoy E, Maycock T, Tignor M, Waterfield T (eds.)]. In Press; 2018.

3. Berg P, Moseley C, Haerter JO. Strong increase in convective precipitation in response to higher temperatures. Nature Geoscience. 2013;6:181–185. doi:10.1038/ngeo1731.

4. Handmer J, Honda Y, Kundzewicz ZW, Arnell N, Benito G, Hatfield J, Mohamed IF, Peduzzi P, Wu S, Sherstyukov B, Takahashi K, Yan Z. Changes in impacts of climate extremes: human systems and ecosystems. In: Managing the Risks of Extreme Events and Disasters to Advance Climate Change Adaptation. Field CB, Barros V, Stocker TF, Qin D, Dokken DJ, Ebi KL, Mastrandrea MD, Mach KJ, Plattner G-K, Allen SK, Tignor M, Midgley PM, editors. A Special Report of Working Groups I and II of the Intergovernmental Panel on Climate Change (IPCC). Cambridge: Cambridge University Press; 2012. p. 231–290.

5. United Nations Framework Convention on Climate Change (UNFCCC). Adoption of the Paris Agreement. FCCC/CP/2015/L.9/Rev.1. 2015.

6. Schleussner CF, Lissner TK, Fischer EM, Wohland J, Perrette M, Golly A, Rogelj J, Childers K, Schewe J, Frieler K, Mengel M, Hare W, Schaeffer M. Differential climate impacts for policy-relevant limits to global warming: the case of 1.5 °C and 2 °C. Earth System Dynamics. 2016;7:327–351. doi:10.5194/esd-7-327-2016.

7. Henley BJ, King AD. Trajectories towards the 1.5 °C Paris target: modulation by the Interdecadal Pacific Oscillation. Geophysical Research Letters. 2017;44:4256–4262. doi:10.1002/2017GL073480.

8. Huntingford C, Mercado L. High chance that current atmospheric greenhouse concentrations commit to warmings greater than 1.5 °C over land. Scientific Reports. 2016;6:30294. doi:10.1038/srep30294.

9. van Vuuren DP, Edmonds J, Kainuma M, et al. The representative concentration pathways: an overview. Climatic Change. 2011;109:5. doi:10.1007/s10584-011-0148-z.

10. Evans J. CORDEX - An international climate downscaling initiative. Modelling and Simulation Society of Australia and New Zealand (MSSANZ), MODSIM2011. 2011;2705–271. doi:10.36334/modsim.2011.f5.evans.

11. Nikulin G, Jones C, Giorgi F, Asrar G, Büchner M, Cerezo-Mota R, Christensen O, Dqu M, Fernández J, Haensler A, Meijgaard E, Samuelsson P, Sylla M, Sushama L. Precipitation climatology in an ensemble of CORDEX-Africa

regional climate simulations. Journal of Climate. 2012 Sep;25:6057–6078. doi:10.1175/JCLI-D-11-00375.1.

12. Kalognomou EA, Lennard C, Shongwe M, Pinto I, Favre A, Kent M, Hewitson B, Dosio A, Nikulin G, Panitz HJ, Büchner M. A diagnostic evaluation of precipitation in CORDEX models over Southern Africa. Journal of Climate. 2013 Jul;26:9477–9506.doi:10.1175/JCLI-D-12-00703.1.

13. Endris HS, Omondi P, Jain S, Lennard C, Hewitson B, Chang'a L, Awange J. Assessment of the performance of CORDEX regional climate models in simulating East African rainfall. Journal of Climate. 2013 Dec;26:8453–8475. DOI: https://doi.org/10.1175/JCLI-D-12-00708.1

14. Mutayoba E, Kashaigili J. Evaluation for the performance of the CORDEX regional climate models in simulating rainfall characteristics over Mbarali River Catchment in the Rufiji Basin, Tanzania. Journal of Geoscience and Environmental Protection. 2017 Jan;5:139–151. doi:10.4236/gep.2017.54011.

15. Warnatzsch E, Reay D. Temperature and precipitation change in Malawi: Evaluation of CORDEX-Africa climate simulations for climate change impact assessments and adaptation planning. Science of The Total Environment. 2018 Nov;654:378–392. doi:10.1016/j.scitotenv.2018.11.098.

16. Ayugi B, Tan G, Gnitou G, Ojara M, Ongoma V. Historical evaluations and simulations of precipitation over East Africa from Rossby Centre Regional Climate Model. Atmospheric Research. 2019 Nov;232:1–17. doi:10.1016/j.atmosres.2019.104705.

17. Demissie T, Sime C. Assessment of the performance of CORDEX regional climate models in simulating rainfall and air temperature over Southwest Ethiopia. Heliyon. 2021 Aug;7:e07791. doi:10.1016/j.heliyon.2021.e07791.

18. Kisembe J, Favre A, Dosio A, Lennard C, Sabiiti G, Nimusiima A. Evaluation of rainfall simulations over Uganda in CORDEX regional climate models. Theoretical and Applied Climatology. 2019 Jul;137:1117–1134. doi:10.1007/s00704-018-2643-x.

19. Zhang X, Alexander L, Hegerl G, Jones P, Tank A, Peterson T, Trewin B, Zwiers F. Indices for monitoring changes in extremes based on daily temperature and precipitation data. Wiley Interdisciplinary Reviews: Climate Change. 2011 Nov;2:851–870. doi:10.1002/wcc.147.

20. Subba S, Ma Y, Ma W. Spatial and temporal analysis of precipitation extremities of Eastern Nepal in the last two decades (1997–2016). Journal of Geophysical Research: Atmospheres. 2019;124:7523–7539. doi:10.1029/2019JD030639.

21. Alexander L, Fowler H, Bador M, Behrangi A, Donat M, Dunn R, Funk C, Goldie J, Lewis E, Rogé M, Seneviratne S, Venugopal V. On the use of indices to study extreme precipitation on sub-daily and daily timescales. Environmental Research Letters. 2019 Dec;14. doi:10.1088/1748-9326/ab51b6.

22. Maure G, Pinto I, Ndebele-Murisa M, Muthige M, Lennard C, Nikulin G, Dosio A, Meque A. The southern African climate under 1.5^0 and 2^0C of global warming as simulated by CORDEX models. Environmental Research Letters. 2018 Jun;13. doi:10.1088/1748-9326/aab190.

23. Pinto I, Lennard C, Tadross M, Hewitson B, Dosio A, Nikulin G, Panitz HJ, Shongwe M. Evaluation and projections of extreme precipitation over southern Africa from two CORDEX models. Climatic Change. 2016 Apr;135:655–668. doi:10.1007/s10584-015-1573-1.

24. Samuel S, Dosio A, Mphale K, Nsadisa Faka D, Wiston M. Comparison of multi-model ensembles of global and regional climate model projections for daily characteristics of precipitation over four major river basins in southern Africa. Part II: Future changes under 1.5 ˚C, 2.0 ˚C and 3.0 ˚C warming levels. Atmospheric Research. 2023;293:106921. doi:10.1016/j.atmosres.2023.106921.

25. Akumaga U, Tarhule A. Projected changes in intra-season rainfall characteristics in the Niger River Basin, West Africa. Atmosphere. 2018 Dec;9:497. doi:10.3390/atmos9120497.

26. Gudoshava M, Misiani H, Tessema Z, Jain S, Ouma J, Otieno G, Indasi VS, Endris HS, Osima SE, Lennard C, Zaroug M, Mwangi E, Nimusiima A, Kondowe A, Ogwang B, Artan G, Atheru Z. Projected effects of 1.5 and 2 °C global warming levels on the intra-seasonal rainfall characteristics over the Greater Horn of Africa. Environmental Research Letters. 2020 Mar;15. doi:10.1088/1748-9326/ab6b33.

27. Makondo C, Thomas D. Seasonal and intra-seasonal rainfall and drought characteristics as indicators of climate change and variability in Southern Africa: a focus on Kabwe and Livingstone in Zambia. Theoretical and Applied Climatology. 2020;140:271–284. doi:10.1007/s00704-019-03029-x.

28. Chabala L, Kuntashula E, Kaluba P. Characterization of temporal changes in rainfall, temperature, flooding hazard and dry spells over Zambia. Universal Journal of Agricultural Research. 2013 Nov;1:134–144. doi:10.13189/ujar.2013.010403.

29. Libanda B, Ngonga C. Projection of frequency and intensity of extreme precipitation in Zambia: A CMIP5 study. Climate Research. 2018 Sep;76:59–72. doi:10.3354/cr01528.

30. Wani SP, Sreedevi TK, Rockström J, Ramakrishna YS. Rainfed agriculture – past trends and future prospects. In: Wani SP, Rockström J, Oweis T, editors. *Rainfed Agriculture: Unlocking the Potential*. Wallingford, UK: CABI; 2009. p. 1–35. (Comprehensive Assessment of Water Management in Agriculture Series: 7). ISBN 9781845933890.

31. Ngoma H, Lupiya P, Kabisa M, Hartley F. Impacts of climate change on agriculture and household welfare in Zambia: an economy-wide analysis. *Climatic Change*. 2021;167:55. doi:10.1007/s10584-021-03168-z.

32. Jain S. An empirical economic assessment of impacts of climate change on agriculture in Zambia. World Bank; 2007. Policy Research Working Paper No. 4291.

33. Couroche K. Climate change in Zambia: impacts and adaptation. Global Majority E-Journal. 2010;1(2):85–96.

34. Geiger R. Klassifikationen der Klimate nach W. Köppen. In: Landolt-Börnstein: Zahlenwerte und Funktionen aus Physik, Chemie, Astronomie, Geophysik und Technik, alte Serie. Vol 3. Berlin: Springer; 1954. p. 603–607.

35. Zambia Seasons - Weather in Zambia. 2021 Apr 20. Available from: https://www.ventureco-worldwide.com/zambia-seasons-weather-in-zambia/

36. United Nations Development Programme (UNDP). Adaptation to the effects of drought and climate change in Agro-ecological Regions I and II in Zambia. Project ID: 3942. PIMS No. 3942.

37. Phiri J, Malec K, Kapuka A, Maitah M, Appiah-Kubi SNK, Gebeltová Z, Bowa M, Maitah K. Impact of agriculture and energy on CO_2 emissions in Zambia. Energies. 2021 Dec;14:8339. doi:10.3390/en14248339.

38. Kasali G. Climate change and health in Zambia. CLACC Working Paper No. 2; 2008.

39. Rudolf B, Becker A, Schneider U, Meyer-Christoffer A, Ziese M. The new “GPCC Full Data Reanalysis Version 5” providing high-quality gridded monthly precipitation data for the global land-surface is public available since December 2010. GPCC Status Report. 2010 Dec;7 p.

40. Nikulin G, Lennard C, Dosio A, Kjellström E, Chen Y, Haensler A, Kupiainen M, Laprise R, Mariotti L, Maule C, Meijgaard E, Panitz HJ, Scinocca J, Somot S. The effects of 1.5 and 2 degrees of global warming on Africa in the CORDEX ensemble. Environmental Research Letters. 2018 Jun;13. doi:10.1088/1748-9326/aab1b1.

41. Taylor KE. Summarizing multiple aspects of model performance in a single diagram. Journal of Geophysical Research. 2001;106:7183–7192. doi:10.1029/2000JD900719.

42. Snider AE, Vasey EH. Probability of wet or dry days in North Dakota. North Dakota Farm Research. 1968 May–Jun;3–5.

43. Nkemelang T, New M, Zaroug M. Temperature and precipitation extremes under current, 1.5 °C and 2.0 °C global warming above pre-industrial levels over Botswana, and implications for climate change vulnerability. Environmental Research Letters. 2018 Jun;13. doi:10.1088/1748-9326/aac2f8.

44. Osima SE, Indasi VS, Zaroug M, Endris HS, Gudoshava M, Misiani H, Nimusiima A, Otieno G, Ogwang B, Jain S, Kondowe A, Mwangi E, Lennard C, Nikulin G, Dosio A. Projected climate over the Greater Horn of Africa under 1.5 °C and 2 °C global warming. Environmental Research Letters. 2018 Jun;13. doi:10.1088/1748-9326/aaba1b.

45. Hachigonta S, Reason CJC. Interannual variability in dry and wet spell characteristics over Zambia. Climate Research. 2006 Aug;32:49–62. doi:10.3354/cr032049.

46. Giorgi F, Coppola E, Raffaele F, Diro G, Fuentes Franco R, Giuliani G, Mamgain A, Llopart M, Mariotti L, Torma C. Changes in extremes and hydroclimatic regimes in the CREMA ensemble projections. Climatic Change. 2014 Jul;125:39–51. doi:10.1007/s10584-014-1117-0.

47. New M, Hewitson B, Stephenson D, Tsiga A, Kruger A, Manhique A, et al. Evidence of trends in daily climate extremes over southern and west Africa. Journal of Geophysical Research. 2006;111:D14102. doi:10.1029/2005JD006289.

48. Shongwe ME, van Oldenborgh GJ, van den Hurk BJJM, de Boer B, Coelho CAS, van Aalst MK. Projected Changes in Mean and Extreme Precipitation in Africa under Global Warming. Part I: Southern Africa. Journal of Climate. 2009;22(13):3819–3837. doi:10.1175/2009JCLI2317.1.

49. Rouault M, Dieppois B, Tim N, Hünicke B, Zorita E. Southern Africa climate over the recent decades: Description, variability and trends. In: von Maltitz GP, Midgley GF, Veitch J, Brümmer C, Rötter RP, Viehberg FA, Veste M, editors. Sustainability of Southern African Ecosystems under Global Change: Science for Management and Policy Interventions. Cham: Springer International Publishing; 2024. p. 149–168. Available from: https://doi.org/10.1007/978-3-031-10948-5_6.

50. Zita LE, Justino F, Gurjão C, Adamu J, Talacuece M. Spatio-temporal characteristics of climate extremes in Sub-Saharan Africa and potential impact of oceanic teleconnections. Atmosphere. 2025;16(1):86. Available from: https://www.mdpi.com/2073-4433/16/1/86.

51. Chemura A, Nangombe SS, Gleixner S, Chinyoka S, Gornott C. Changes in Climate Extremes and Their Effect on Maize (*Zea mays* L.) Suitability Over Southern Africa. Front Clim. 2022;4:890210. doi:10.3389/fclim.2022.890210.

52. Ayanlade A, Oluwaranti A, Ayanlade OS, Borderon M, Sterly H, Sakdapolrak P, et al. Extreme climate events in sub-Saharan Africa: A call for improving agricultural technology transfer to enhance adaptive capacity. Climate Services. 2022;27:100311. doi:10.1016/j.cliser.2022.100311.

53. Stadtbäumer C, Ruesink B, Gronau S. Climate change scenarios in Zambia: modeling farmers' adaptation. Agriculture & Food Security. 2022;11:52. doi:10.1186/s40066-022-00382-5.

54. Bobde V, Akinsanola AA, Folorunsho AH, Adebiyi AA, Adeyeri OE. Projected regional changes in mean and extreme precipitation over Africa in CMIP6 models. *Environmental Research Letters*. 2024;19(7):074009. doi:10.1088/1748-9326/ad545c.

55. Munday C, Washington R, Engelstaedter S, Zilli M, Harbord S, Knight C, Attwood K, Hart N. Southern African climate change: processes, models, and projections. *WIREs Climate Change*. 2025 Sep;16(5). doi:10.1002/wcc.70025.

56. Addisu AA, Tsidu GM, Basupi LV. Improving daily CMIP6 precipitation in Southern Africa through bias correction—Part 2: representation of extreme precipitation. *Climate*. 2025;13(5):93. doi:10.3390/cli13050093.

57. Liapapa C, Shi J, Kamukama Ebaju G, Adongo Obuo M, Friday Hakabinga A, Zobanya Hamisi E, Niyigena T. Inter-model diversity among CMIP6 models in simulating summer precipitation over Zambia. *Atmospheric and Oceanic Science Letters*. 2026 May;100860. doi:10.1016/j.aosl.2026.100860.

58. World Weather Attribution. El Niño key driver of drought in highly vulnerable Southern African countries. 2024 Apr. Available from: `https://www.worldweatherattribution.org/el-nino-key-driver-of-drought-in-highly-vulnerable-southern-african-count`

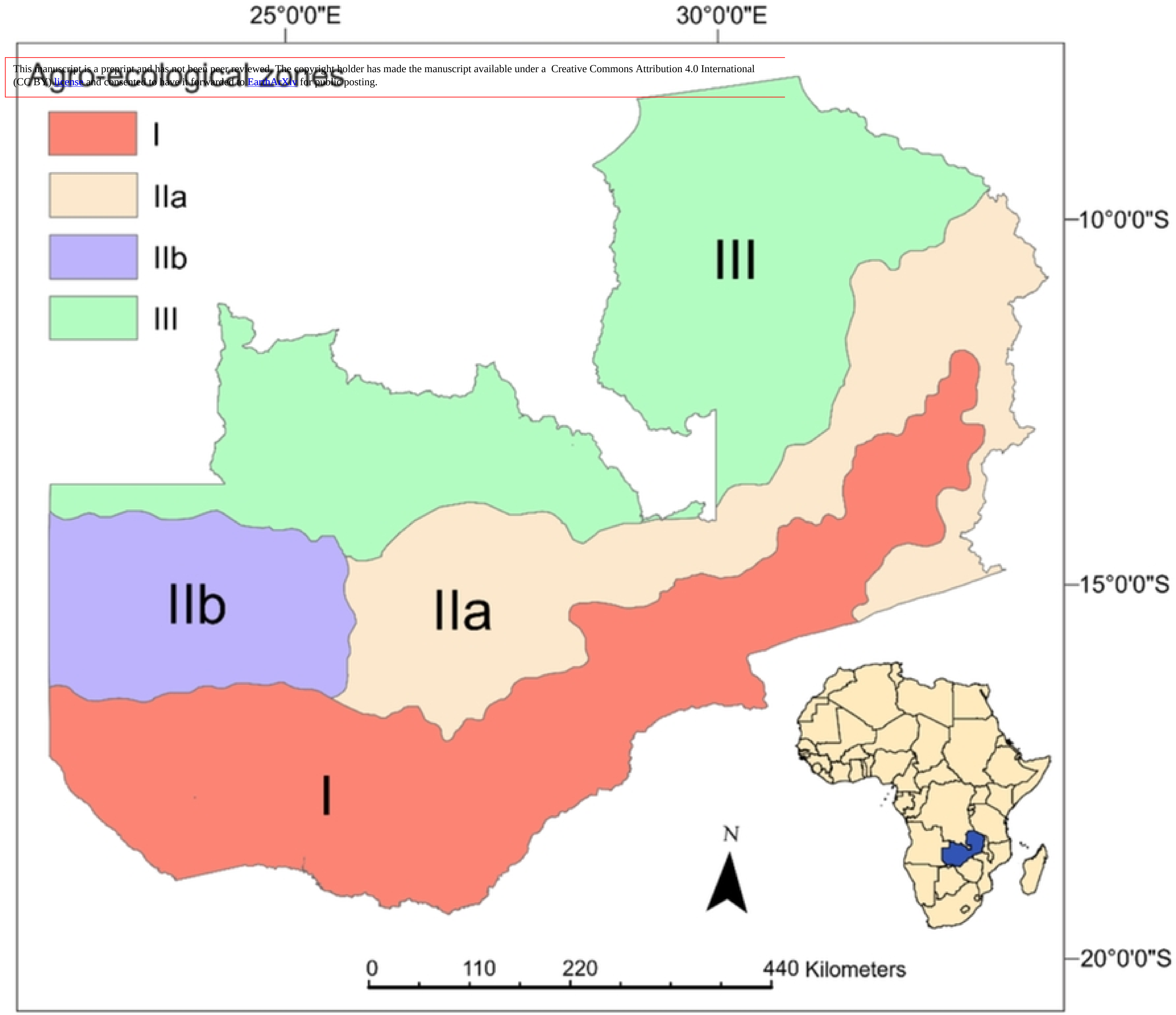
25°0'0"E
30°0'0"E
Agro-ecological zones
I
IIa
IIb
III
III
IIb
IIa
I
10°0'0"S
15°0'0"S
20°0'0"S
N
0
110
220
440 Kilometers

Figure

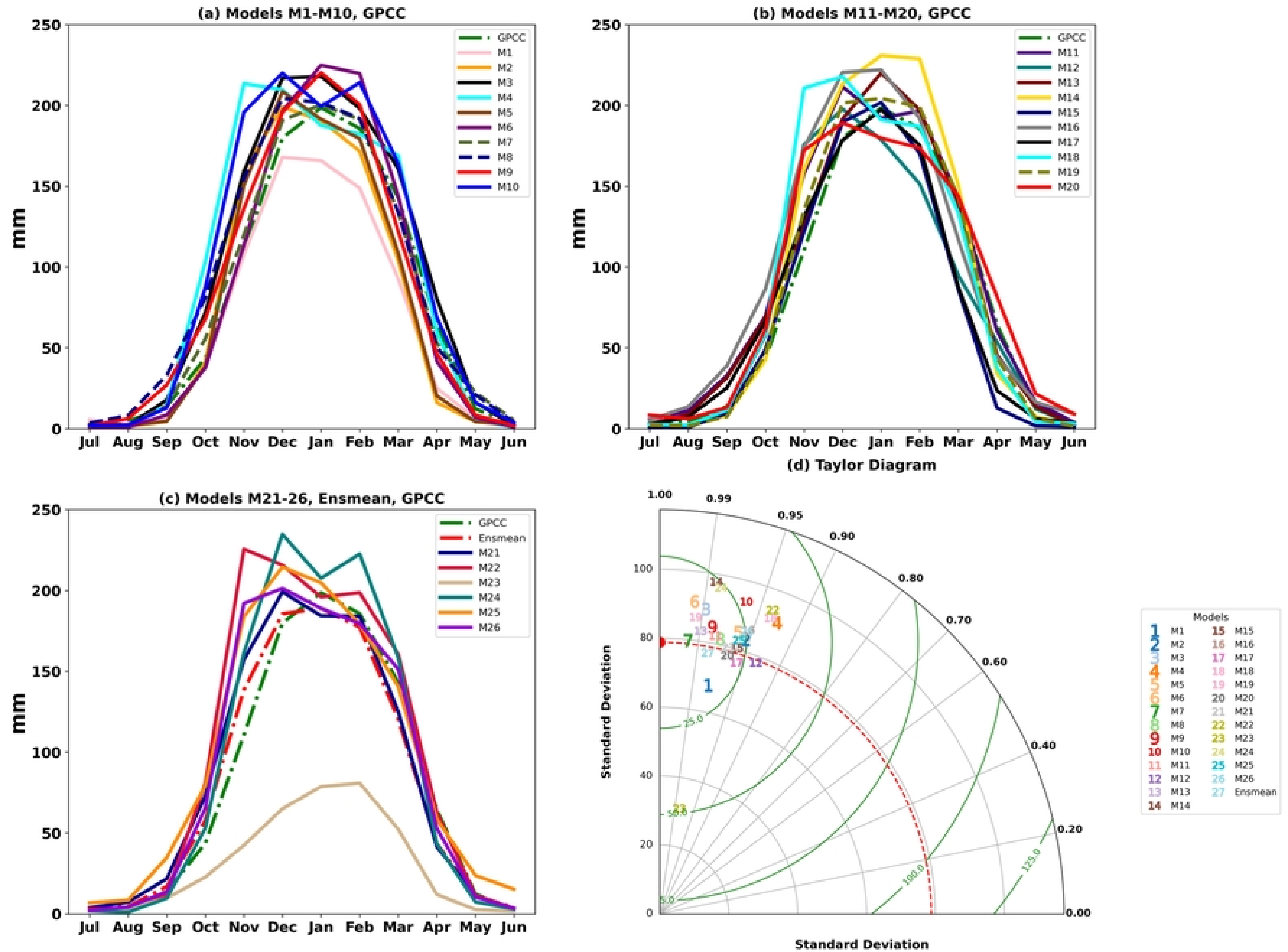

(a) Models M1-M10, GPCC
(b) Models M11-M20, GPCC
(c) Models M21-26, Ensmean, GPCC
(d) Taylor Diagram
mm
Jul
Aug
Sep
Oct
Nov
Dec
Jan
Feb
Mar
Apr
May
Jun
GPCC
Ensmean
Standard Deviation
Models

Figure

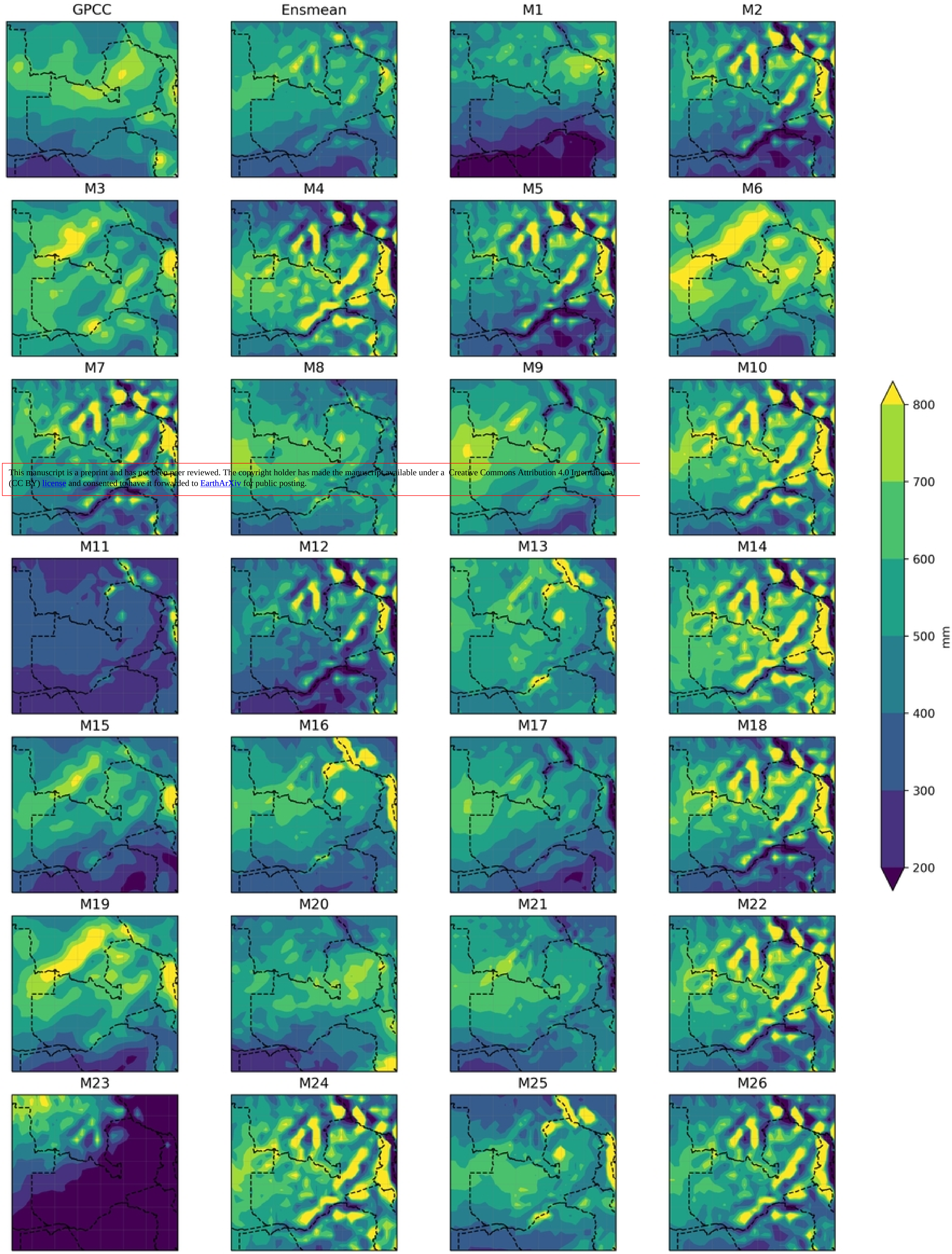
GPCC
Ensmean
M1
M2
M3
M4
M5
M6
M7
M8
M9
M10
M11
M12
M13
M14
M15
M16
M17
M18
M19
M20
M21
M22
M23
M24
M25
M26
800
700
600
500
400
300
200
mm

Figure

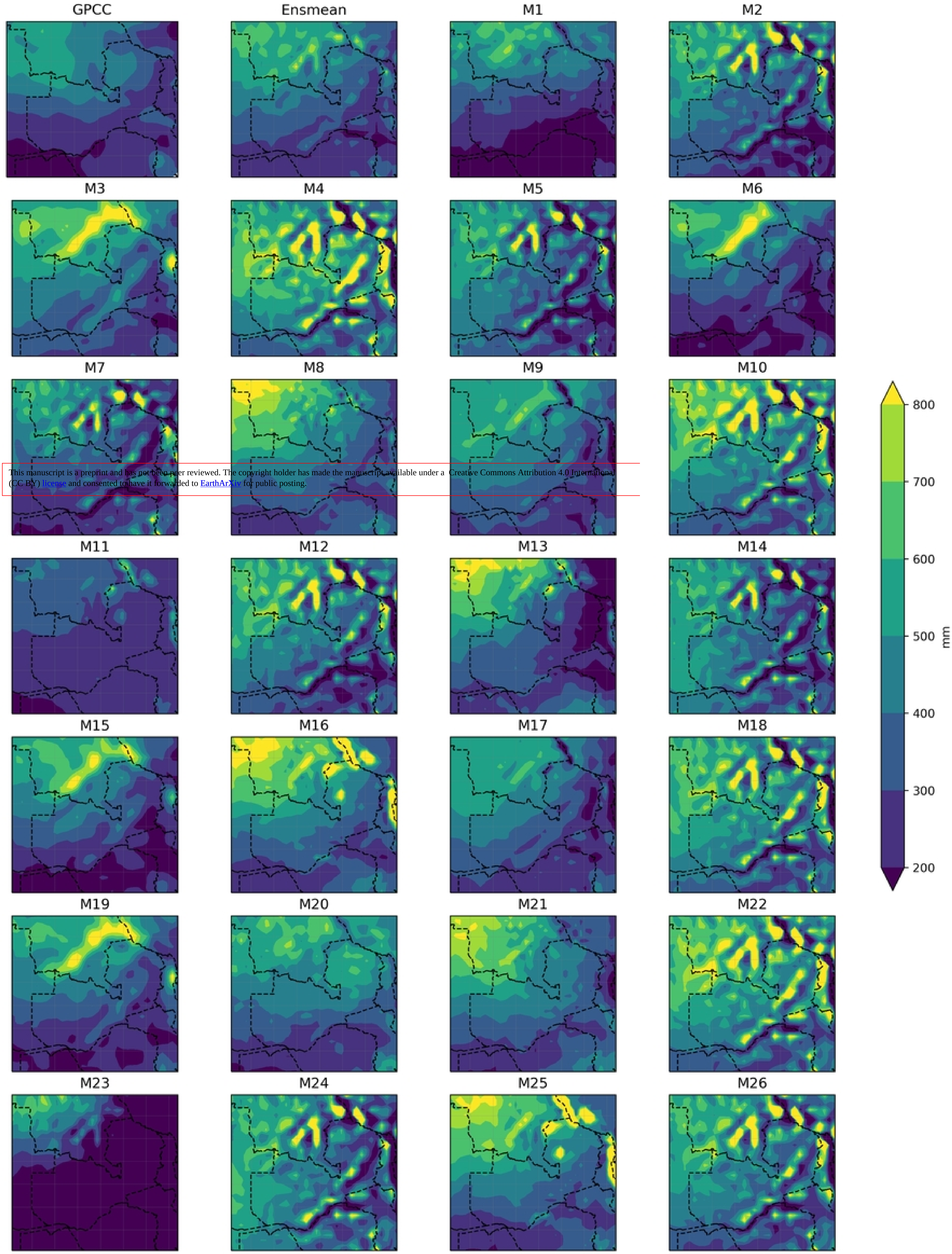
GPCC
Ensmean
M1
M2
M3
M4
M5
M6
M7
M8
M9
M10
M11
M12
M13
M14
M15
M16
M17
M18
M19
M20
M21
M22
M23
M24
M25
M26
800
700
600
500
400
300
200
mm

Figure

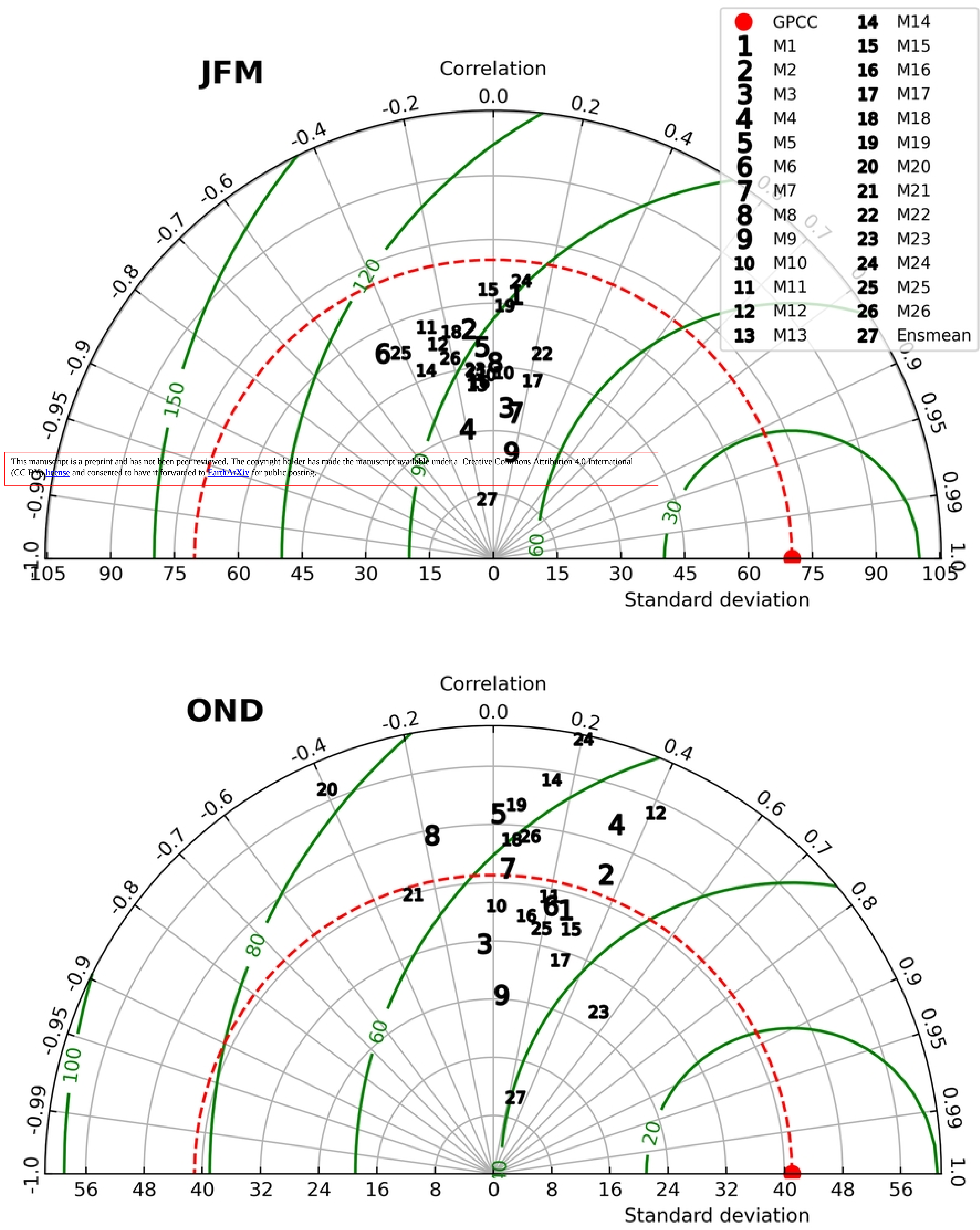
JFM
OND
Correlation
Standard deviation
GPCC
M1
M2
M3
M4
M5
M6
M7
M8
M9
M10
M11
M12
M13
M14
M15
M16
M17
M18
M19
M20
M21
M22
M23
M24
M25
M26
Ensmean

Figure

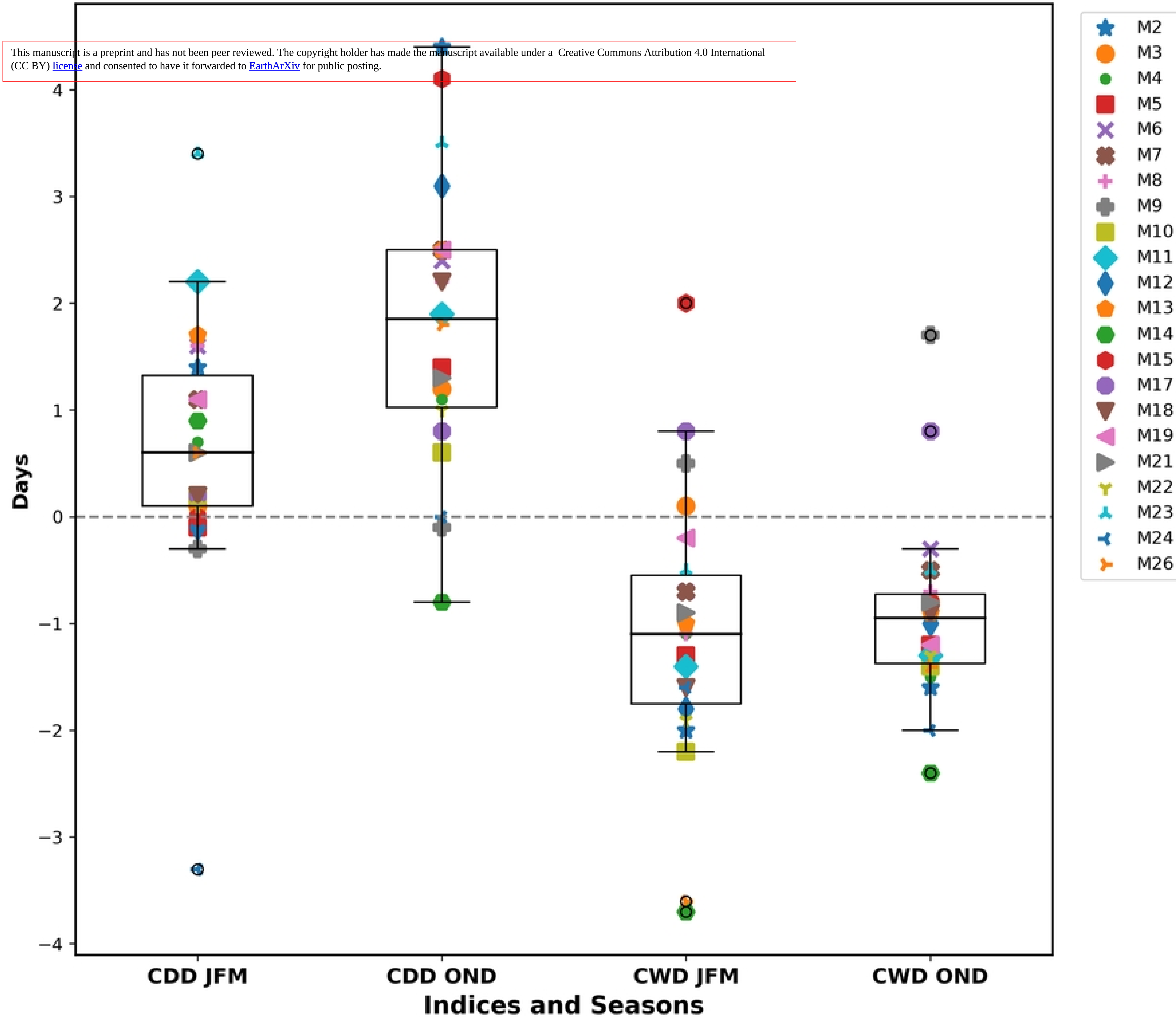
Days
4
3
2
1
0
−1
−2
−3
−4
CDD JFM
CDD OND
CWD JFM
CWD OND
Indices and Seasons
M2
M3
M4
M5
M6
M7
M8
M9
M10
M11
M12
M13
M14
M15
M17
M18
M19
M21
M22
M23
M24
M26

Figure

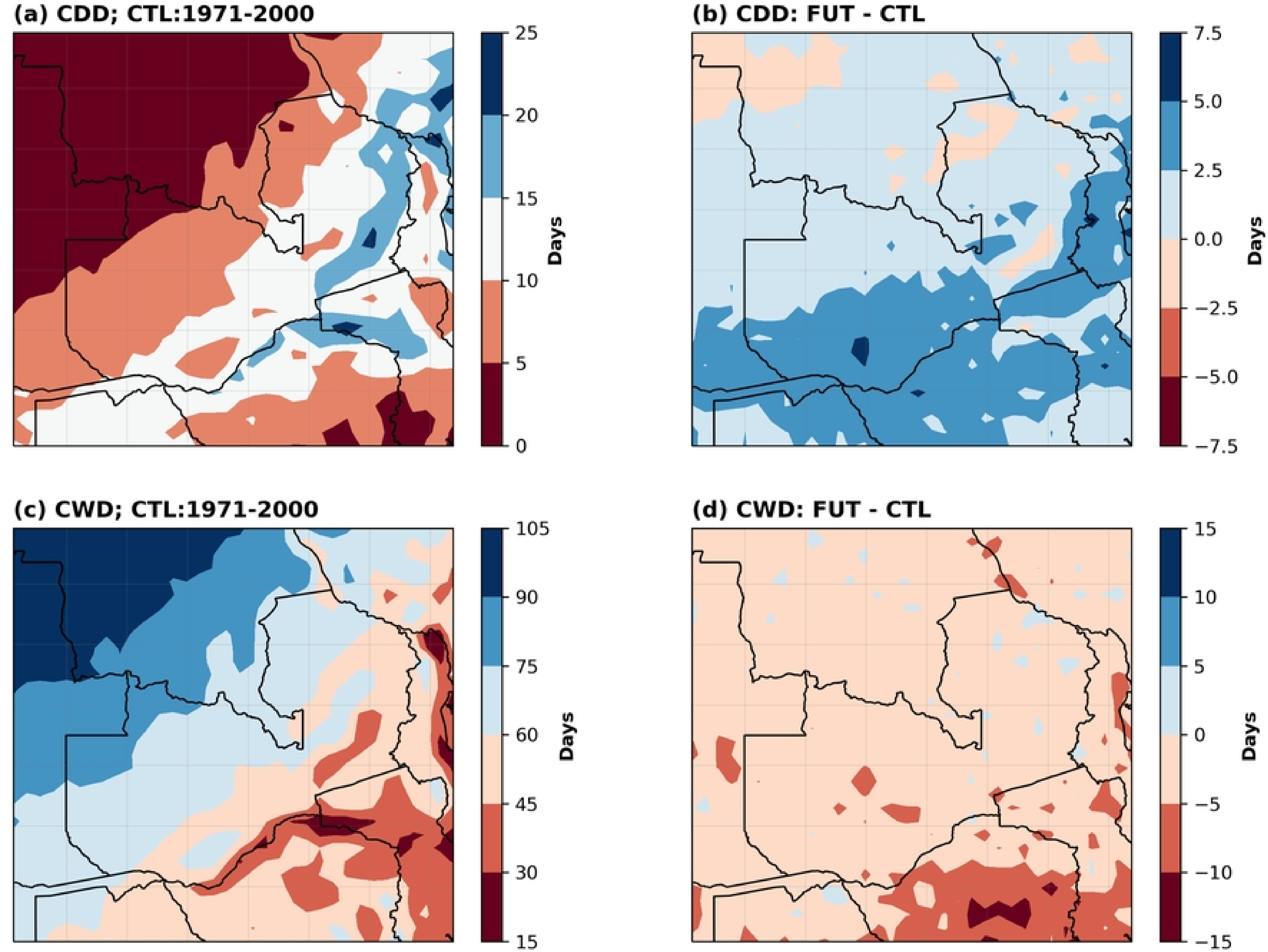
(a) CDD; CTL:1971-2000
25
20
15
10
5
0
Days
(b) CDD: FUT - CTL
7.5
5.0
2.5
0.0
−2.5
−5.0
−7.5
Days
(c) CWD; CTL:1971-2000
105
90
75
60
45
30
15
Days
(d) CWD: FUT - CTL
15
10
5
0
−5
−10
−15
Days

Figure

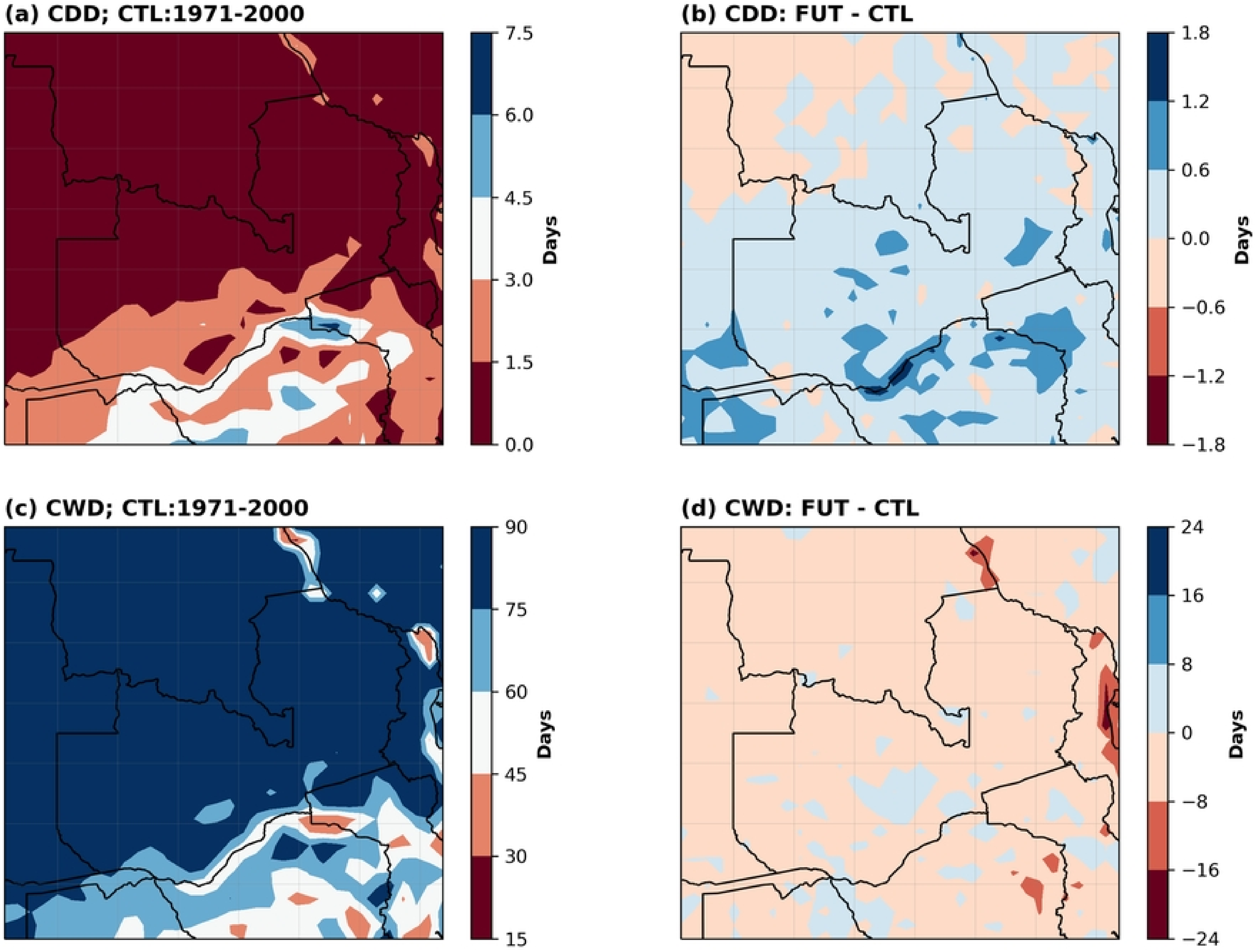
(a) CDD; CTL:1971-2000
(b) CDD: FUT - CTL
(c) CWD; CTL:1971-2000
(d) CWD: FUT - CTL
Days
7.5
6.0
4.5
3.0
1.5
0.0
1.8
1.2
0.6
0.0
−0.6
−1.2
−1.8
90
75
60
45
30
15
24
16
8
0
−8
−16
−24

Figure